J|A|C|S COMMUNICATIONS

Published on Web 10/09/2009

Single-Site, Catalytic Water Oxidation on Oxide Surfaces

Zuofeng Chen, Javier J. Concepcion, Jonah W. Jurss, and Thomas J. Meyer*

Department of Chemistry, University of North Carolina at Chapel Hill, Chapel Hill, North Carolina 27599

Received July 30, 2009; E-mail: tjmeyer@unc.edu

Notable progress has recently been made in identifying single-site catalysts for water oxidation including detailed mechanism elucidation.[1−5] This includes water oxidation by $[Ru(tpy)(bpm)(OH_2)]^{2+}$ and $[Ru(tpy)(bpz)(OH_2)]^{2+}$ (tpy = 2,2′:6′,2″-terpyridine; bpm = 2,2′-bipyrimidine; bpz = 2,2′-bipyrazine) by the mechanism in Scheme 1.[1] For applications in electrocatalysis or photoelectrocatalysis, transferring solution reactivity to conducting or semiconductor solution interfaces is important to accelerate rates and minimize catalyst in a device configuration.[6] We report here electrocatalytic water oxidation by a surface-bound complex that functions on conducting and semiconducting oxide surfaces, retains the solution mechanism on the surface, and provides a basis for sustained, electrocatalytic water oxidation over a range of pH values.

Scheme 1. Mechanism of Water Oxidation by the Single-Site Catalysts $[Ru(tpy)(bpm)(OH_2)]^{2+}$ and $[Ru(tpy)(bpz)(OH_2)]^{2+}$

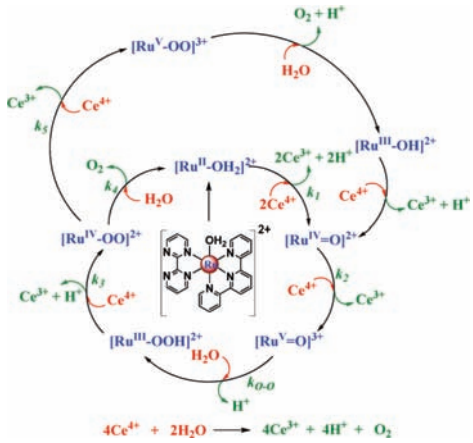

Syntheses of the water oxidation catalyst $[Ru(Mebimpy)(bpy)(OH_2)]^{2+}$ (**1**) [Mebimpy = 2,6-bis(1-methylbenzimidazol-2-yl)-pyridine; bpy = 2,2′-bipyridine] and $[Ru(Mebimpy)(4,4′-((HO)_2OPCH_2)_2bpy)(OH_2)]^{2+}$ (**1-PO$_3$H$_2$**) (Figure 1) have been reported elsewhere.[7] In these reactions, $Ru(Mebimpy)Cl_3$ was allowed to react with bpy or 4,4′-$((EtO)_2OPCH_2)_2$bpy in 2:1 EtOH/H_2O in the presence of NEt_3, giving $[Ru(Mebimpy)(L)(Cl)]^+$ [L = bpy or 4,4′-$((EtO)_2OPCH_2bpy)$]. The chloride ligand was subsequently displaced by the more labile triflate anion in neat triflic acid. Upon addition of water, rapid aquation occurred, and the resulting aqua complex was isolated as the triflate salt by addition of excess lithium triflate. For the phosphonate ester precursor of **1-PO$_3$H$_2$** [L = 4,4′-$((EtO)_2OPCH_2)_2$bpy], the ester groups were hydrolyzed by heating the complex in 4.0 M aqueous HCl at 100 °C for 4 days prior to replacement of the chloride ligand.

Stable phosphonate surface binding of **1-PO$_3$H$_2$** on fluorine-doped SnO_2 (FTO) or Sn(IV)-doped In_2O_3 (ITO) and in optically transparent films (∼10 μm thickness) of TiO_2 nanoparticles (10−20 nm diameter) prepared by a literature procedure[8] on FTO (FTO|TiO_2) occurred following exposure of the electrodes to a 0.1 mM stock solution of **1-PO$_3$H$_2$** in methanol. Saturation coverage of 1.2×10^{-10} mol/cm^2 on FTO and ITO was achieved in ∼2 h, as monitored by the area under the cyclic voltammetric wave for the Ru(III/II) couple at $E_{1/2}$ = 0.67 V vs NHE at pH 5 (CH_3CO_2H/CH_3CO_2Na buffer, I = 0.1 M) (Figure S1 in the Supporting Information). The extent of surface loading on FTO|TiO_2 (in mol/cm^2) was calculated from UV−vis measurements using the expression $\Gamma = A(\lambda)/[10^3\varepsilon(\lambda)]$, where $A(\lambda)$ and $\varepsilon(\lambda)$ are the absorbance and molar absorptivity at wavelength λ.[9] For surface-bound $Ru^{II}-OH_2^{2+}$, λ_{max} = 493 nm, and $\varepsilon_{max} = 1.5 \times 10^4$ M^{-1} cm^{-1} for **1-PO$_3$H$_2$** in methanol were used for $\varepsilon(\lambda)$. Typical saturated surface coverages after 4 h exposure times were 5.3×10^{-8} mol/cm^2 for FTO|TiO_2 (Figure S2).

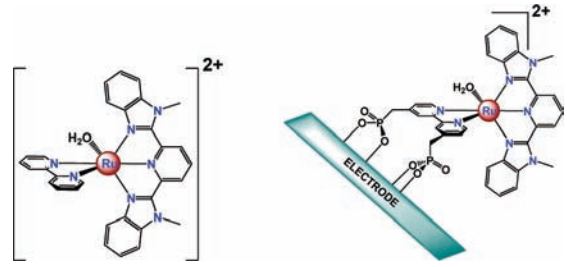

Figure 1. Structure of **1** and schematic representation of **1-PO$_3$H$_2$** attached to a metal oxide electrode.

Figure 2a shows a cyclic voltammogram (CV) of FTO|**1-PO$_3$H$_2$** at pH 5 (CH_3CO_2H/CH_3CO_2Na buffer, I = 0.1 M). As for the solution couples in Figures S3 and S4, pH-dependent waves appear for sequential Ru(III/II) and Ru(IV/III) couples on the surface at ∼0.67 and 0.98 V. The peak currents vary with scan rate, as expected for surface couples. A pH-independent Ru(V/IV) wave appears at ∼1.67 V at the onset of a catalytic water oxidation wave. Closely related results were obtained for ITO|**1-PO$_3$H$_2$** (Figure S5). As observed earlier for a related surface couple, the $Ru^{IV}=O^{2+}/Ru^{III}-OH^{2+}$ wave is kinetically inhibited on the surface as a result of the proton demands of the couple.[10] It is more distinct at slow scan rates or high pH (Figure S4). Plots of $E_{1/2}$ versus pH for solution and surface couples are shown in Figures S6 and S7.

The catalytic peak current at 1.85 V varies linearly with surface coverage (Figure S8), consistent with a single-site mechanism for water oxidation. The scan-rate-normalized catalytic peak current (i/v) increases with decreasing scan rate, consistent with a rate-limiting step prior to electron transfer to the electrode (Figure S9).

Stepping the applied potential to $E_{p,a}$ = 1.85 V at pH 5 results in sustained electrocatalytic water oxidation (Figure 2b) with a current density of ∼14.8 μA/cm^2. Catalysis was sustained for at least 8 h, corresponding to ∼11 000 turnovers at a turnover rate of ∼0.36 s^{-1}. Sustained catalytic currents were also obtained at pH 1 (0.1 M HNO_3) with a current density of ∼4.9 μA/cm^2 (Figure S10).

10.1021/ja906391w CCC: $40.75 © 2009 American Chemical Society

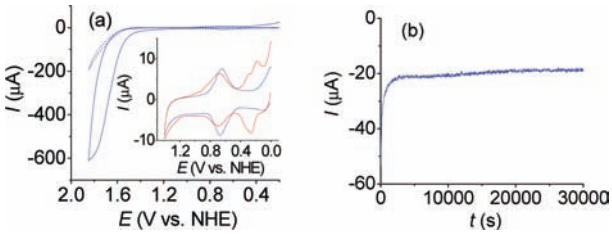

Figure 2. (a) CVs of FTO|**1-PO$_3$H$_2$** at pH 5 (I = 0.1 M, CH_3CO_2H/CH_3CO_2Na buffer; scan rate 100 mV/s). The dotted line is the FTO background under the same experimental conditions. The inset shows CVs of FTO|**1-PO$_3$H$_2$** at pH 5 before (blue line) and after (red line) scanning to 1.85 V. (b) Electrolysis of FTO|**1-PO$_3$H$_2$** at 1.85 V vs NHE at pH 5. Number of turnovers ≈ 11 000, turnover frequency ≈ 0.36 s^{-1} (background subtracted). $\Gamma = 1.2 \times 10^{-10}$ mol/cm^2, area = 1.25 cm^2, current density ≈ 14.8 μA/cm^2.

The surface catalyst was also investigated on FTO|TiO_2. The same pattern of voltammetric waves was observed (Figure S11). In CVs, the peak current for the Ru(III/II) couple varied linearly with the square root of the scan rate (Figure S12). This is consistent with an earlier observation for a surface-bound Os^{II} complex[9] and electron transfer to and from the surface couple by cross-surface electron transfer. On the basis of peak current measurements, ∼2.5 and ∼8.0% of the available sites were electroactive at scan rates of 100 and 10 mV/s, respectively. Complete oxidation occurs on longer time scales. As shown in Figure 3, the spectrum of FTO|TiO_2|**1-PO$_3$H$_2$** is dominated by a metal-to-ligand charge transfer (MLCT) absorption band at 493 nm as $Ru^{II}-OH_2$. A potential-hold experiment at 0.75 V at pH 5 (past $E_{1/2}$ for the $Ru^{III}-OH^{2+}/Ru^{II}-OH_2^{2+}$ couple) resulted in spectral changes consistent with oxidation of $Ru^{II}-OH_2^{2+}$ to $Ru^{III}-OH^{2+}$, and at 1.20 V, oxidation of $Ru^{III}-OH^{2+}$ to $Ru^{IV}=O^{2+}$. A further increase in potential to 1.85 V resulted in spectral features for an intermediate similar to $Ru^{IV}=O^{2+}$, presumably, $Ru^{IV}(OO)^{2+}$ (see below and Scheme 1). Reduction of $Ru^{III}-OH^{2+}$ or $Ru^{IV}=O^{2+}$ past $E_{p,c}$ for the $Ru^{III}-OH^{2+}/Ru^{II}-OH_2^{2+}$ couple resulted in complete recovery of $Ru^{II}-OH_2^{2+}$.

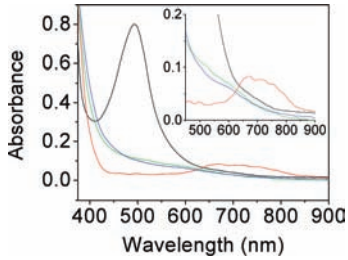

Figure 3. UV−vis spectra of FTO|TiO_2|**1-PO$_3$H$_2$** (black line), following complete electrolysis at 0.75 V (red line, actual spectrum × 4.5), 1.20 V (green line), and 1.85 V (blue line) vs NHE at pH 5. The spectrum in red was obtained with $\Gamma = 0.26 \times 10^{-10}$ mol/cm^2 and the others with $\Gamma = 1.2 \times 10^{-10}$ mol/cm^2. The inset shows a magnified view of the low-energy spectrum.

The complex retains its electrocatalytic activity toward water oxidation on FTO|TiO_2. Electrolysis of FTO|TiO_2|**1-PO$_3$H$_2$** at 1.85 V at pH 5 resulted in sustained electrocatalysis (Figure S13). Water oxidation is slow on FTO|TiO_2|**1-PO$_3$H$_2$**, with a turnover rate of 0.004 s^{-1}, because of rate-limiting cross-surface electron transfer.[9] Comparison of the integrated current over a period of 30 000 s with the results of in situ measurement of O_2 evolution by an oxygen electrode (YSI ProODO) gave 6.5 μmol of O_2, corresponding to an oxygen yield of 77%. In view of the difficulties in the experiment, this represents a lower limit yield.

There is additional insight into the mechanism in the surface experiments. In Scheme 1, the key O−O bond-forming step is H_2O attack on the oxo group of $Ru^V=O^{3+}$. Following an oxidative scan through the catalytic wave at $E_{p,a}$ = 1.85 V for FTO|**1-PO$_3$H$_2$** at pH 5, new waves appear at $E_{1/2}$ = 0.30 and 0.22 V (Figure 2a inset). Both waves are pH-dependent (Figure S7). These observations are consistent with a surface peroxidic intermediate and the couples in eq 1:

$$Ru^{IV}(OO)^{2+} + e^- + H^+ \rightarrow Ru^{III}-OOH^{2+} \quad (1a)$$

$$Ru^{III}-OOH^{2+} + e^- + H^+ \rightarrow Ru^{II}(HOOH)^{2+} \quad (1b)$$

After the potential was held for 10 min at 1.85 V, the initial spectrum of $Ru^{II}-OH_2^{2+}$ on FTO|TiO_2|**1-PO$_3$H$_2$** with λ_{max} = 493 nm shifted to 595 nm. This is consistent with formation of $Ru^{IV}(OO)^{2+}$ with λ_{max} = 598 nm for the analogous solution intermediate $[Ru^{IV}(Mebimpy)(bpy)(OO)]^{2+}$ from an earlier kinetic study.[5] After the solution was left to stand at pH 5 for 12 h, the initial spectrum of $Ru^{II}-OH_2^{2+}$ was completely recovered. This is consistent with O_2 evolution by the surface analogue of the k_4 step in Scheme 1. The time for recovery of the $Ru^{II}-OH_2^{2+}$ spectrum was reduced to <40 min by bubbling Ar through the solution or mechanically perturbing the slide.

Our observations are striking in revealing that the surface-bound complex retains its chemical properties ($E_{1/2}$ values, pH dependence) and physical properties (UV−vis spectra), including its ability to catalyze water oxidation. Significantly, electrocatalysis also occurs on TiO_2, which has been used extensively in dye-sensitized solar cells.[11,12]

Acknowledgment. Funding support for this research by the Chemical Sciences, Geosciences, and Biosciences Division of the Office of Basic Energy Sciences, U.S. Department of Energy (DE-FG02-06ER15788), is gratefully acknowledged.

Supporting Information Available: Coverage-time dependence for **1-PO$_3$H$_2$** adsorbed on the oxide surfaces, surface-coverage dependence of the catalytic peak current, scan-rate dependences, electrochemical studies of solution couples, and surface-bound couples at ITO|**1-PO$_3$H$_2$** and FTO|TiO_2|**1-PO$_3$H$_2$**, and $E_{1/2}$-versus-pH plots for the solution and surface-bound couples. This material is available free of charge via the Internet at http://pubs.acs.org.

References

(1) Concepcion, J. J.; Jurss, J. W.; Templeton, J. L.; Meyer, T. J. *J. Am. Chem. Soc.* **2008**, *130*, 16462.
(2) McDaniel, N. D.; Coughlin, F. J.; Tinker, L. L.; Bernhard, S. *J. Am. Chem. Soc.* **2008**, *130*, 210.
(3) Tseng, H.-W.; Zong, R.; Muckerman, J. T.; Thummel, R. *Inorg. Chem.* **2008**, *47*, 11763.
(4) Hull, J. F.; Balcells, D.; Blakemore, J. D.; Incarvito, C. D.; Eisenstein, O.; Brudvig, G. W.; Crabtree, R. H. *J. Am. Chem. Soc.* **2009**, *131*, 8730.
(5) Concepcion, J. J.; Tsai, M.-K.; Muckerman, J. T.; Meyer, T. J. *J. Am. Chem. Soc.*, in revision.
(6) Liu, F.; Cardolaccia, T.; Hornstein, B. J.; Schoonover, J. R.; Meyer, T. J. *J. Am. Chem. Soc.* **2007**, *129*, 2446.
(7) Concepcion, J. J.; Jurss, J. W.; Norris, M. R.; Templeton, J. L.; Meyer, T. J. *Inorg. Chem.*, in revision.
(8) Heimer, T. A.; D'Arcangelis, S. T.; Farzad, F.; Stipkala, J. M.; Meyer, G. J. *Inorg. Chem.* **1996**, *35*, 5319.
(9) Trammell, S. A.; Meyer, T. J. *J. Phys. Chem. B* **1999**, *103*, 104.
(10) Trammell, S. A.; Wimbish, J. C.; Odobel, F.; Gallagher, L. A.; Narula, P. M.; Meyer, T. J. *J. Am. Chem. Soc.* **1998**, *120*, 13248.
(11) Grätzel, M. *Inorg. Chem.* **2005**, *44*, 6841.
(12) Argazzi, R.; Murakami Iha, N. Y.; Zabri, H.; Odobel, F.; Bignozzi, C. A. *Coord. Chem. Rev.* **2004**, *248*, 1299.

JA906391W